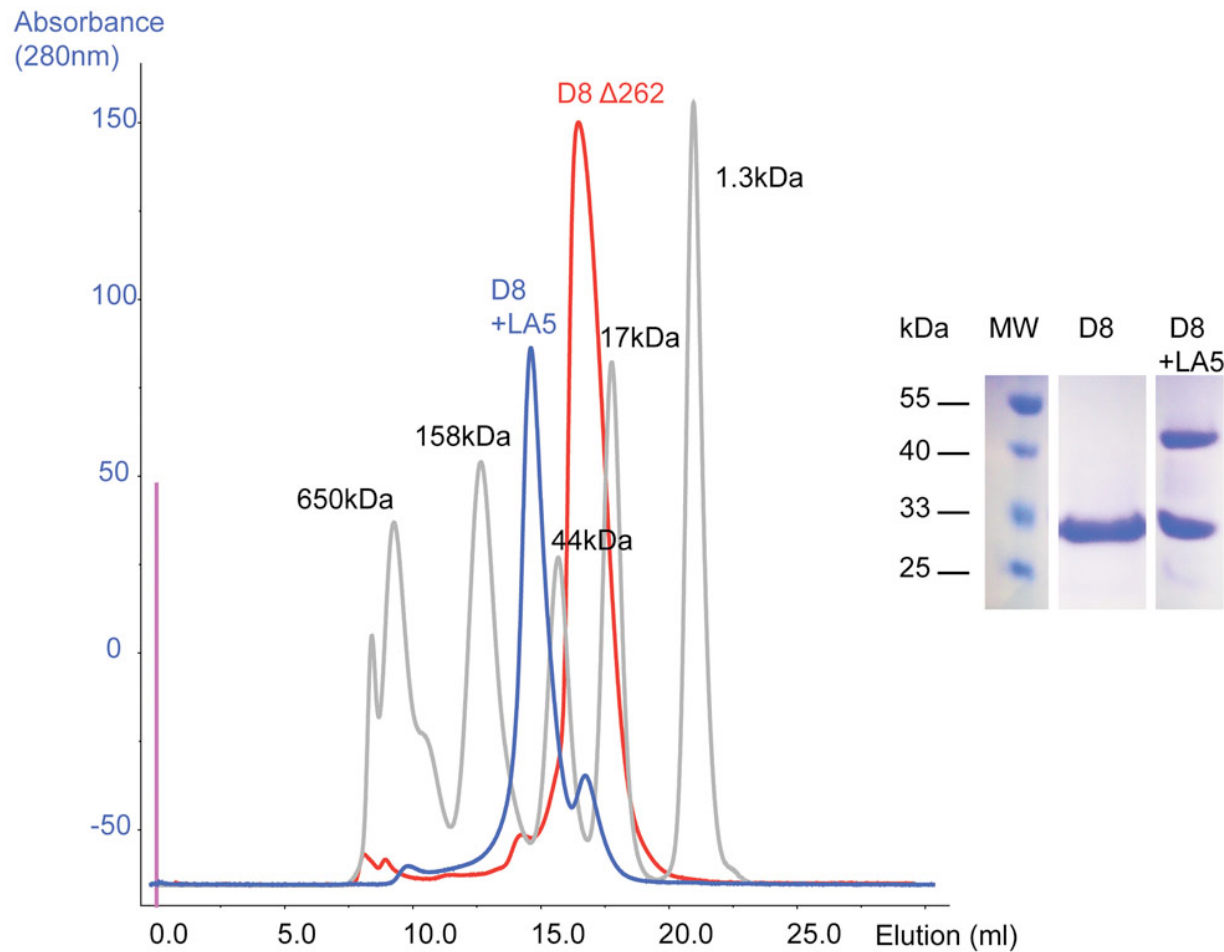
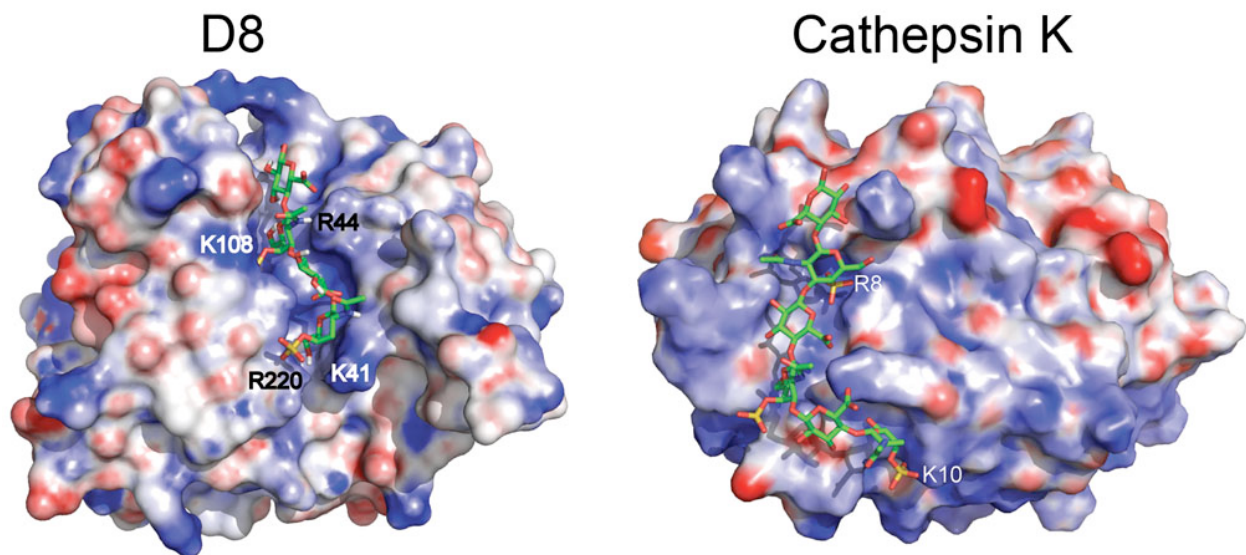


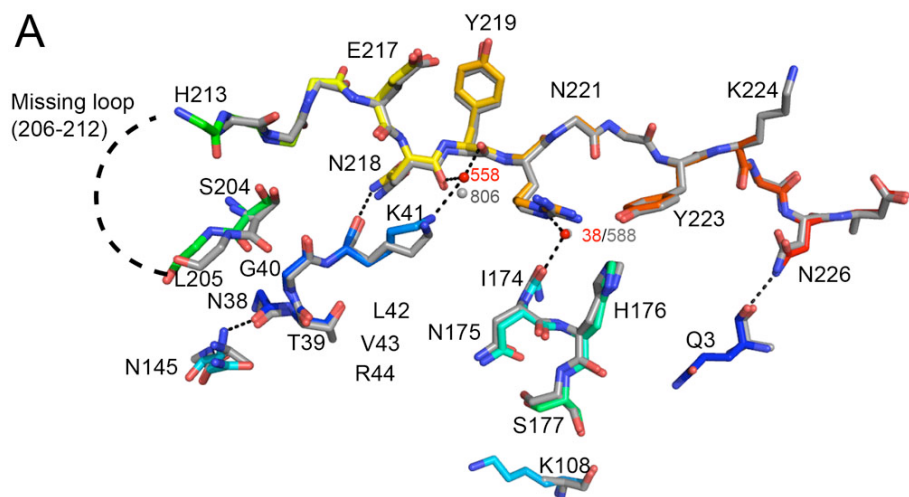
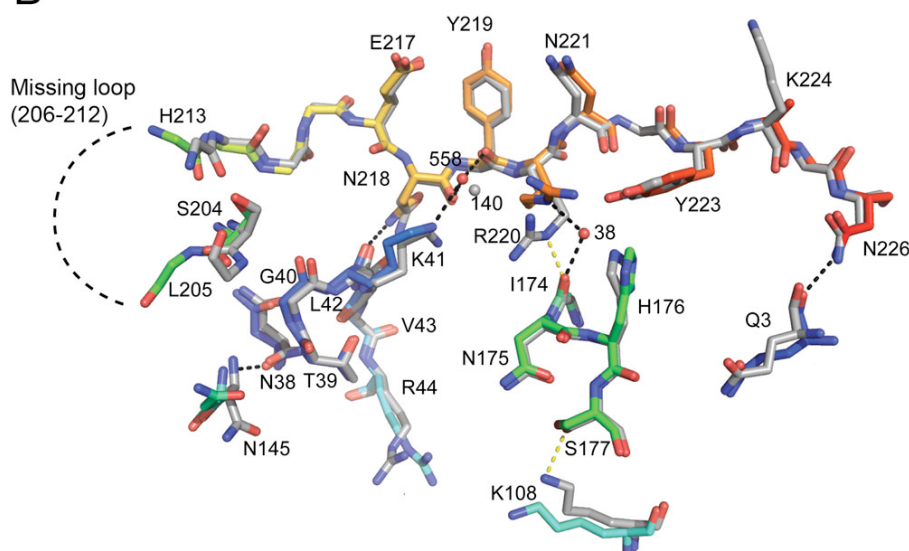
## Supporting Material



**Figure S1. D8/LA5-Fab complex formation.** Size exclusion chromatography (SEC) of monomeric D8 (red trace) and the D8/LA5 complex (blue trace). Profile of MW standard markers are shown in grey with size indicated. Inset shows SDS-PAGE for both SEC peaks. The D8/LA5 complex has an apparent MW of ~80 kDa, as expected by theoretical MWs of individual proteins and SDS-PAGE shows two distinct bands for D8 and LA5 (inset, right lane).



**Figure S2. Docking top score maps CS tetrasaccharide binding site to D8 electropositive crevice.** The top C4S/D8 docking solution is shown (left), compared to the CS binding site of the complex structure of CS/cathepsin K (right).

**A****B**

**Figure S3. Comparison of the D8L before and after LA5 binding .** (A) D8L conformational epitopes of both molecules in the asymmetric unit of the D8 only crystal (chain C and X) were superimposed. Epitope subregion definition is the same as in Fig. 6A. Chain X is represented in rainbow and chain C in grey. Water molecules 38, 558 (red) and 588, 806 (grey) are represented. RMSD = 0.37 Å. Electron density is missing for K224X, K108C and N145C. Side chains are shown for antigenic residues, and when they serve in overall epitope integrity (N218, N226). (B) Comparison of D8 epitope forming residues before (grey) and after (colored) binding to the antibody LA5.

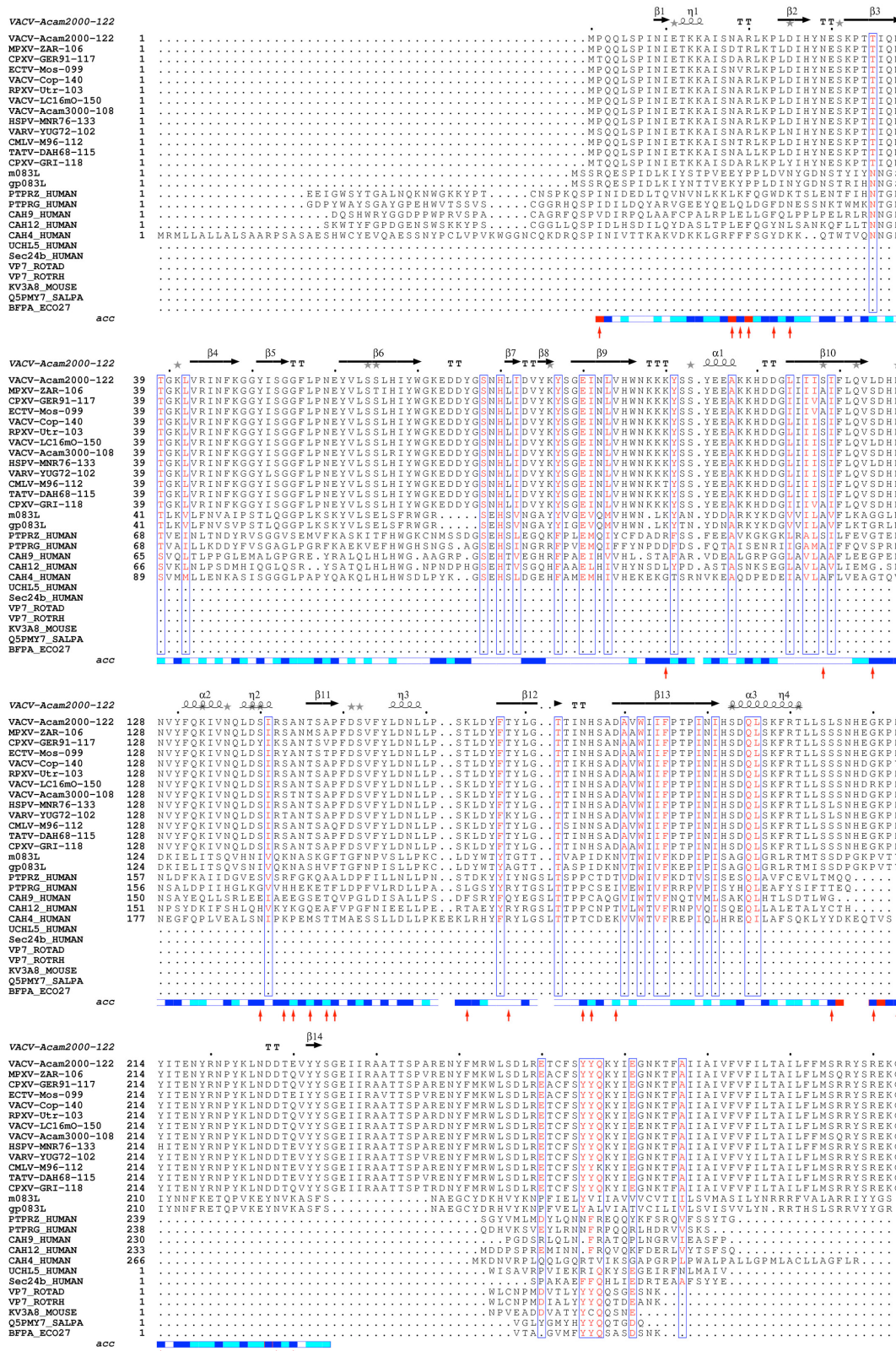


**Figure S4. VACV-Acam2000 D8 sequence alignment and residue accessibility.** The entire D8 sequence was aligned to the most relevant CA domain homologues using ClustalW (6), along with homologues for the smaller, C-terminal extra-viral domain (Vp7-like). D8 secondary structure is represented on top of the alignment, as extracted by ESPRIPT (3) using DSSP (4). CA-like homologues include orthopox and more distant MYXV and RFV representatives (m083L and gp083L), human carbonic anhydrases (CAH) 4, 9, and 12, and extra-cytoplasmic anchoring domains of PTPRs. Initial MR model that led to D8 structure was built using PTPR $\zeta$  as template. VACV: vaccinia; VARV: variola; HSPV: horsepox virus; CMLV: camelpox virus; MPXV: monkeypox virus; MYXV: myxoma virus ; CPXV: cowpox virus; ECTV: ectromelia virus; RFV: rabbit fibroma virus; RPXV: rabbitpox virus; RFV Rabbit fibroma virus; TATV: taterapox virus. For the smaller Vp7-like domain, only the relevant matching sequence of the protein was aligned as follows: UchL5 196-224, Sec24b 1234-1257, Vp7 rotavirus glycoproteins ROTAD and ROTRH 163-183, KV38A 80-97, Q5PMY7 68-83, and BFPA 29-45. Cysteine 262 is conserved throughout the orthopox homologues. Relative accessibility of each residue is extracted from DSSP (4) and is rendered as blue-colored boxes located at the bottom of the alignment. Cyan- and white-colored boxes report intermediary and buried residues, respectively. Red-colored boxes highlight residues for which accessibility is not predicted due side-chains being stubbed. Red arrows point out the variation spectrum residues of the D8L orthopox family (refer to Fig. 7 and Table S5).

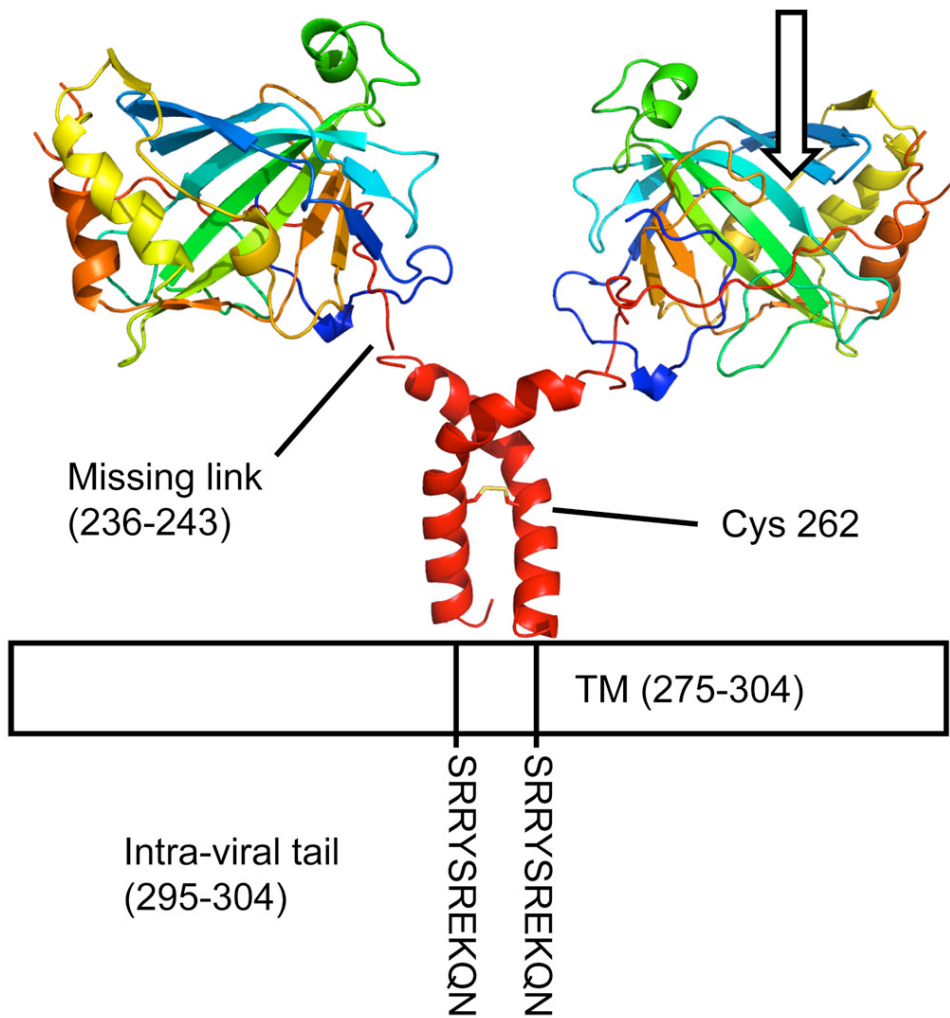


**Figure S5. Model of the covalent full-length D8 dimer.** Both Sec24b and Uch37, represented in the alignment (Fig. S4), were used to model the region 244-274 of full-length D8. Both human proteins present 42% identity to D8 over residues 244-269 and 254-282, respectively. The predicted TM of D8 was not included in the model because Uch37 is not a transmembrane protein and therefore does not bear a TM in this region. The representation of the homodimer interface relies purely on the intermolecular disulfide bond formation between both unique cysteines 262 from each molecule. The arrow points to the putative CS-binding site and to the overall D8/LA5-Fab interface. The D8 tetramer was not modeled, due to lack of information on this interface.

**Table S1. Data collection and refinement statistics.**

<b>Data collection statistics</b>	<b>D8 Δ262</b>	<b>LA5-Fab</b>	<b>LA5/D8 Δ262</b>
Space group	p4 <sub>1</sub>	p2 <sub>1</sub> 2 <sub>1</sub> 2 <sub>1</sub>	p2 <sub>1</sub>
Cell dimension			
a, b, c, (Å)	71.3,71.3,44.2	36.2,93.4,136.0	76.0,91.2, 103.8
α, β, γ (°)	90.0,90.0,90.0	90.0,90.0,90.0	90.0,107.3,90.0
Resolution range (Å)	40.00-3.50	31.12-1.60	40.00-2.10
[outer shell]	[1.45-1.42]	[1.69-1.60]	[2.18-2.10]
No. of reflections	40635	56672	75612
R <sub>merge</sub> (%)	6.8 [63.0]	4.8 [32.3]	8.6 [45.9]
Multiplicity	2.0 [2.0]	5.5 [5.1]	3.1 [3.0]
Average I/σI	33.6 [2.7]	17.7 [3.9]	20.7 [2.4]
Completeness (%)	99.5 [100]	96.6 [93.8]	97.8 [93.2]
<b>Refinement statistics</b>			
No. atoms	2179	3818	10825
Protein	1961	3387	10290
Waters	206	410	495
Organic	0	14	22
Inorganic	12	7	16
Ramachandran plot (%)			
Favored	97.35	98.6	97.21
Allowed	100	99.8	99.9
R.m.s. deviations			
Bonds (Å)	0.011	0.012	0.008
Angles (°)	1.350	1.467	1.137
B-factors (Å <sup>2</sup> )			
Protein	18.4	23.8	42.6
Waters	30.5	30.4	40.1
Organic	/	18.3	44.3
Inorganic	25.4	16.0	55.1
R factor (%)	17.38	19.82	20.14
R <sub>free</sub> (%)	18.99	22.87	25.24

[numbers in parenthesis] refer to highest resolution shell

**Table S2. Contacts between LA5-Fab and D8.**

CDR	LA5 residue		Atom	D8 residue		Atom	d(Å)	Angle	Type
L1	Ser 31B	OG		Lys 224X	CB	3.93		VdW	
	<b>Tyr 32L</b>	<b>Arom. ring</b>		<b>Lys 224C</b>	<b>Cation</b>				<b>Cation-pi</b>
L3	Trp 91B	O		Leu 5X	CD1	3.66		VdW	
	Thr 92B	C		Leu 5X	CD1	3.8		VdW	
	Thr 92B	O		Leu 5X	CD1	3.43		VdW	
				Leu 5X	CG	3.77		VdW	
	Tyr 94B	CZ		His 176X	CB	3.87		VdW	
				His 176X	ND1	3.55		VdW	
	<b>Tyr 94B</b>	<b>OH</b>		His 176X	CB	3.61		VdW	
				His 176X	CG	3.56		VdW	
				<b>His 176X</b>	<b>ND1</b>	<b>2.74</b>	***	<b>H-bond</b>	
				His 176X	CE1	3.75		VdW	
	Tyr 94B	CE2		His 176X	CB	3.72		VdW	
				His 176X	CG	3.84		VdW	
				His 176X	ND1	3.52		VdW	
				Leu 5X	CD2	3.74		VdW	
	Tyr 94B	CD2		Leu 5X	CD2	3.8		VdW	
H1	Ser 29A	CA		Leu 205X	CD2	3.9		VdW	
	Ser 29A	CB		Ser 204X	OG	3.52		VdW	
				Ser 204X	O	3.79		VdW	
	<b>Ser 29A</b>	<b>OG</b>		Leu 205X	CG	3.69		VdW	
				Leu 205X	CD2	3.57		VdW	
				<b>Ser 204X</b>	<b>OG</b>	<b>2.66</b>	***	<b>H-bond</b>	
				Ser 204X	C	3.85		VdW	
				Ser 204X	CB	3.63		VdW	
				Ser 204X	O	3.53		VdW	
	Asn 31A	CB		Thr 39X	O	3.68		VdW	
	Asn 31A	CG		Thr 39X	O	3.89		VdW	
				Asn 145X	OD1	3.92		VdW	
	<b>Asn 31A</b>	<b>ND2</b>		Asn 145X	ND2	3.99	*	VdW	
				<b>Thr 39X</b>	<b>O</b>	<b>3.16</b>	***	<b>H-bond</b>	
				Asn 145X	CG	3.68		VdW	
				<b>Asn 145X</b>	<b>OD1</b>	<b>2.77</b>	***	<b>H-bond</b>	
	Phe 32A	CA		Lys 41X	CD	3.9		VdW	
	Phe 32A	CG		Lys 41X	CD	3.64		VdW	
	Phe 32A	CD1		Gly 40X	O	3.22		VdW	
				Ser 204X	CB	4		VdW	
				Lys 41X	CD	3.58		VdW	
	Phe 32A	CE1		Ile 215X	CG2	3.66		VdW	
				Gly 40X	O	3.65		VdW	
				Lys 41X	CD	3.63		VdW	
	Phe 32A	CZ		Glu 217X	O	3.09		VdW	
				Lys 41X	CD	3.72		VdW	
	Phe 32A	CE2		Glu 217X	O	3.77		VdW	

			Lys	41X	CD	3.77	VdW	
			Lys	41X	CE	3.88	VdW	
Phe	32A	CD2	Lys	41X	CD	3.73	VdW	
			Lys	41X	CE	3.85	VdW	
Phe	32A	C	Lys	41X	CE	3.99	VdW	
Phe	32A	O	Lys	41X	CD	3.6	VdW	
			Lys	41X	CE	3.09	VdW	
<b>Phe</b>	<b>32A</b>	<b>Arom. ring</b>	<b>Lys</b>	<b>41X</b>	<b>Cation</b>		<b>Cation-pi</b>	
Trp	34A	CZ3	His	176X	ND1	3.94	VdW	
Trp	34A	CH2	Arg	220X	CZ	3.9	VdW	
			Arg	220X	NH2	3.78	VdW	
			Ile	174X	O	3.86	VdW	
			Asn	175X	CA	3.97	VdW	
			Asn	175X	C	3.93	VdW	
			Asn	175X	O	3.81	VdW	
			His	176X	ND1	3.82	VdW	
Trp	34A	CZ2	Ile	174X	O	3.75	VdW	
			Asn	175X	CA	3.51	VdW	
			Asn	175X	C	3.96	VdW	
			Asn	175X	O	3.93	VdW	
<b>Trp</b>	<b>34A</b>	<b>Arom. ring</b>	<b>Arg</b>	<b>220X</b>	<b>Cation</b>		<b>Cation-pi</b>	
<b>H2</b>	Met	51A	CE	Asn	175X	O	3.55	VdW
				His	176X	CB	3.89	VdW
Asp	53A	CB	Asn	175X	ND2	3.9	VdW	
<b>Asp</b>	<b>53A</b>	<b>OD2</b>	Asn	175X	CB	3.64	VdW	
			Asn	175X	CG	3.98	VdW	
			<b>Asn</b>	<b>175X</b>	<b>ND2</b>	<b>3.29</b>	***	<b>H-bond</b>
Ser	55A	CA	Thr	39X	O	3.8	VdW	
Ser	55A	CB	Thr	39X	O	3.29	VdW	
			Thr	39X	OG1	3.79	VdW	
Ser	55A	OG	Thr	39X	OG1	4	*	VdW
Glu	56A	CD	Arg	44X	NH1	3.29	VdW	
Glu	56A	OE1	Thr	39X	CG2	3.97	VdW	
			Arg	44X	NH1	3.61	*	SALT
<b>Glu</b>	<b>56A</b>	<b>OE2</b>	<b>Arg</b>	<b>44X</b>	<b>NH1</b>	<b>3.02</b>	***	<b>SALT</b>
			Arg	44X	NE	4.44	*	SALT
Glu	58A	CB	Asn	175X	ND2	3.77	VdW	
			Ser	177X	OG	3.73	VdW	
Glu	58A	CG	Lys	108X	NZ	3.54	VdW	
Glu	58A	CD	Asn	175X	ND2	3.81	VdW	
			Ser	177X	OG	3.98	VdW	
			Lys	108X	CE	3.89	VdW	
			Lys	108X	NZ	3.62	VdW	
<b>Glu</b>	<b>58A</b>	<b>OE1</b>	Asn	175X	CG	3.61	VdW	
			Asn	175X	OD1	3.78	*	VdW
			<b>Asn</b>	<b>175X</b>	<b>ND2</b>	<b>2.65</b>	***	<b>H-bond</b>
<b>Glu</b>	<b>58A</b>	<b>OE2</b>	Ser	177X	OG	3.43	*	H-bond
			Lys	108X	CE	3.31	VdW	
			<b>Lys</b>	<b>108X</b>	<b>NZ</b>	<b>3.01</b>	***	<b>SALT</b>

	Ser	59A	O	Ser	177X	CB	3.92	VdW
	Arg	60A	CD	His	176X	O	3.48	VdW
				Ser	177X	O	3.93	VdW
	Arg	60A	CZ	His	176X	O	3.98	VdW
				Gln	3X	OE1	3.46	VdW
	<b>Arg</b>	<b>60A</b>	<b>NH1</b>	<b>His</b>	<b>176X</b>	<b>O</b>	<b>2.94</b>	<b>*** H-bond</b>
				Gln	3X	CD	3.73	VdW
				Gln	3X	OE1	3.08	*** H-bond
				Gln	3X	NE2	3.63	*
	<b>Arg</b>	<b>60A</b>	<b>NH2</b>	Gln	3X	CD	3.72	VdW
				<b>Gln</b>	<b>3X</b>	<b>OE1</b>	<b>2.96</b>	<b>*** H-bond</b>
				Gln	3X	NE2	3.8	*
	Arg	75A	CB	Asn	145X	OD1	3.96	VdW
	Arg	75A	CD	Asn	145X	OD1	3.3	VdW
<b>H3</b>	Asn	101A	O	Arg	220X	NH1	3.95	*
	Tyr	102A	CE1	Glu	217X	OE2	3.73	VdW
	Tyr	102A	CZ	Glu	217X	OE2	3.63	VdW
	<b>Tyr</b>	<b>102A</b>	<b>OH</b>	<b>Glu</b>	<b>217X</b>	<b>OE2</b>	<b>2.67</b>	<b>*** H-bond</b>
				Glu	217X	CG	3.82	VdW
				Glu	217X	CD	3.54	VdW
	Tyr	102A	C	Arg	220X	NH1	3.59	VdW
	<b>Tyr</b>	<b>102A</b>	<b>O</b>	<b>Arg</b>	<b>220X</b>	<b>NH1</b>	<b>2.97</b>	<b>*** H-bond</b>
				Arg	220X	CD	3.53	VdW
	Arg	103A	CG	Asn	221X	ND2	4	VdW
	Arg	103A	CD	Asn	221X	OD1	3.75	VdW
				Asn	221X	CG	3.75	VdW
				Asn	221X	ND2	3.52	VdW
	<b>Arg</b>	<b>103A</b>	<b>NE</b>	Tyr	219X	CE1	3.79	VdW
				<b>Tyr</b>	<b>219X</b>	<b>O</b>	<b>3.09</b>	<b>*** H-bond</b>
	Arg	103A	CZ	Glu	217X	CD	3.8	VdW
				Glu	217X	OE1	3.3	VdW
				Tyr	219X	CD1	3.97	VdW
				Tyr	219X	CE1	3.6	VdW
				Tyr	219X	CZ	3.47	VdW
				Tyr	219X	OH	3.84	VdW
				Tyr	219X	CE2	3.73	VdW
				Tyr	219X	O	3.49	VdW
	<b>Arg</b>	<b>103A</b>	<b>NH1</b>	Glu	217X	OE2	3.57	*
				Glu	217X	CD	3.38	VdW
				<b>Glu</b>	<b>217X</b>	<b>OE1</b>	<b>2.75</b>	<b>*** SALT</b>
				Tyr	219X	CE1	3.79	VdW
				Tyr	219X	CZ	3.3	VdW
				Tyr	219X	OH	3.21	*** H-bond
				Tyr	219X	CE2	3.7	VdW
	<b>Arg</b>	<b>103A</b>	<b>NH2</b>	Glu	217X	OE2	3.99	*
				Glu	217X	CG	3.81	VdW
				Glu	217X	CD	3.35	VdW
				<b>Glu</b>	<b>217X</b>	<b>OE1</b>	<b>2.98</b>	<b>*** SALT</b>
				Tyr	219X	CG	3.76	VdW

		Tyr	219X	CD1	3.96	VdW	
		Tyr	219X	CE1	3.93	VdW	
		Tyr	219X	CZ	3.7	VdW	
		Tyr	219X	CE2	3.47	VdW	
		Tyr	219X	CD2	3.5	VdW	
		Tyr	219X	N	3.63	*	
		Tyr	219X	C	3.9	VdW	
		Tyr	219X	O	3.06	***	
Arg	103A	O	Asn	221X	ND2	3.73	VdW
					<b>Arom.</b>		
<b>Arg</b>	<b>103A</b>	<b>Cation</b>	<b>Tyr</b>	<b>219X</b>	<b>ring</b>		<b>Cation-pi</b>
Asp	105A	CG	Arg	220X	NH2	3.9	VdW
			Tyr	223X	OH	3.39	VdW
<b>Asp</b>	<b>105A</b>	<b>OD1</b>	Arg	220X	NH1	3.94	*
			Arg	220X	CZ	3.86	VdW
			<b>Arg</b>	<b>220X</b>	<b>NH2</b>	<b>2.93</b>	***
			Tyr	223X	OH	3.21	***
<b>Asp</b>	<b>105A</b>	<b>OD2</b>	Arg	220X	NH2	4.1	*
			Tyr	223X	CE1	3.27	VdW
			Tyr	223X	CZ	3.35	VdW
			<b>Tyr</b>	<b>223X</b>	<b>OH</b>	<b>2.82</b>	***
							<b>H-bond</b>

The contact list was erected using CCP4i/CONTACT (1) (chains A, B and X). Contact nature determination was constrained by distances requirements ( $d < 3.5 \text{ \AA}$  for hydrogen bonds;  $d < 4 \text{ \AA}$  for VdW interactions;  $d < 4.5 \text{ \AA}$  for salt bridges). Cation-pi contacts were identified using the web-based version of the CaPTURE program (2). Additional contacts that exist only between chains H, L and C are listed in italic. Predominant electrostatic contacts are listed in bold when multiple atoms may compete for the same contact.

**Table S3. Contact summary between D8 and LA5 Fab**

CDR	H-bond	Salt bridge	VdW	Water-mediated	Cation-pi	BSA (Å <sup>2</sup> )
H1:	3	0	43	1	2	646
H2:	6	4	32	2	0	698
H3:	7	7	40	14	1	528
Total:	16	11	115	17	3	1872
L1:	0	0	1	2	1	225
L3:	1	0	15	3	0	337
Total:	1	0	16	5	1	562

Cation-pi contacts were identified using the web-based version of the CaPTURE program (<http://capture.caltech.edu/>) (2), while buried surface areas (BSA) where calculated using PISA ([http://www.ebi.ac.uk/msd-srv/prot\\_int/pistart.html](http://www.ebi.ac.uk/msd-srv/prot_int/pistart.html)) (5).

**Table S4. Bridging waters between LA5-Fab and D8.**

CDR	Residue	Distance	Angle	Water	Distance	Angle	D8 residue
L1	S31B OG	2.87	***	173	3.38	*	K224X N
					2.90	***	K224X O
L3	T92B O	2.94	***	181	3.41	*	N226X OD1
		2.61	***	561	2.45	***	Q3X O
	Y94B N	2.79	***	560	2.52	***	Q3X OE1
H1	W34A NE1	3.46	*	555	3.03	***	K41X NZ
H2	S55A OG	2.74	***	236	2.68	***	T39X OG1
	E56A OE1	3.50	*				
H3	N101A O	2.77	***	35	2.73	***	R220X NH1
					3.44	*	R220X NH2
	Y102A O	3.14	***	555	3.03	***	K41X NZ
		2.70	***	558	2.76	***	Y219X O
					3.03	***	K41X NZ
					3.19	***	N218X O
	R103A O	2.82	***	263	2.78	***	N221X N
					3.23	***	R220X NE
					3.31	*	R220X NH1
		2.69	***	396	2.88	***	N221X ND2
	Y104A O	2.93	***	35	2.73	***	R220X NH1
					3.44	*	R220X NH2
	D105A OD1	2.71	***	35	2.73	***	R220X NH1
					3.44	*	R220X NH2

The contact list was calculated using CCP4i/CONTACT (1) and show every water molecules that elicit hydrogen bonds ( $d < 3.5 \text{ \AA}$ ) with both chain X (D8) and chains A (heavy) or B (light) of LA5-Fab.

**Table S5. D8 sequence variations in orthopox family.**

Variable	Acam2000	Other	Ratios, per	Grouping
2	P	S, T	27:56:3	🍎 ⊖
18	N	D	74:12	🍎
19	A	T, V	78:5:2	🍎
20	R	L	85:1	•
23	P	T	77:9	🍎
25	D	N, Y	66:29:1	🍎
100	K	T	84:2	•
118	S	A	72:14	🍎
124	L	S	10:75	🍎 ⊖
140	S	Y	85:1	•
143	S	T, Y	28:56:2	🍎 ⊖
144	A	T	85:1	•
146	T	M	77:9	🍎
148	A	V, T	82:2:2	•
149	P	Q	84:2	•
163	K	T	74:14	🍎
168	T	K	30:56	🍎 ⊖
175	<b>N</b>	<b>K</b>	<b>85:1</b>	•
176	<b>H</b>	<b>N</b>	<b>84:2</b>	•
179	D	N	84:2	•
<b>205</b>	<b>L</b>	<b>S</b>	<b>60:26</b>	🍎
210	G	R	84:2	•
213	H	Y	85:1	•
214	Y	H	85:1	•
228	D	N	84:2	•
230	E	Q, D	65:19:2	🍎
246	A	V, T	66:19:1	🍎
261	T	A, V	73:7:6	🍎
268	Q	K	84:2	•
272	G	E	82:4	•
293	F	L	9:75	🍎 ⊖
296	R	Q	76:10	🍎

Variations were characterized based on whether they are seldom or secluded within a single orthopox genera (•), whether the considered mutations are comparably represented (🍎), or if a residue of Acam2000 (*i.e.* our D8) sequence does not represent the consensus (⊖). Cases filled in grey are of residues that are not in the structure and therefore are not represented in figure 7. Residues in bold form direct contacts with the antibody LA5. The variation ratios consider every D8L sequence of the PBR independent of its viral origin and are weighed by the number of

isolates of each strain. As a consequence, common variations in strains such as VARV or VACV that constitute the majority of poxvirus sequences in the PBR could be overrepresented.

## References:

1. **CCP4**. 1994. Collaborative Computational Project, Number 4. The CCP4 Suite: Programs for Protein Crystallography. *Acta Crystallogr. D* **50**:760-763.
2. **Gallivan, J. P., and D. A. Dougherty**. 1999. Cation-pi interactions in structural biology. *Proc Natl Acad Sci U S A* **96**:9459-9464.
3. **Gouet, P., E. Courcelle, D. I. Stuart, and F. Metoz**. 1999. ESPript: analysis of multiple sequence alignments in PostScript. *Bioinformatics* **15**:305-308.
4. **Kabsch, W., and C. Sander**. 1983. Dictionary of protein secondary structure: pattern recognition of hydrogen-bonded and geometrical features. *Biopolymers* **22**:2577-2637.
5. **Krissinel, E., and K. Henrick**. 2007. Inference of macromolecular assemblies from crystalline state. *J Mol Biol* **372**:774-797.
6. **Thompson, J. D., D. G. Higgins, and T. J. Gibson**. 1994. CLUSTAL W: improving the sensitivity of progressive multiple sequence alignment through sequence weighting, position-specific gap penalties and weight matrix choice. *Nucleic Acids Res* **22**:4673-4680.